Annu. Rev. Mater. Res. 2001. 31:387–404

SYNTHETIC CELLS–SELF-ASSEMBLING POLYMER MEMBRANES AND BIOADHESIVE COLLOIDS

Daniel A Hammer and Dennis E Discher
School of Engineering and Applied Science, University of Pennsylvania, Philadelphia, PA 19104; e-mail: hammer@seas.upenn.edu

Key Words polymer vesicles, biocolloids, artificial cells

■ **Abstract** We summarize developments in the construction of synthetic cells made from polymers, with a particular focus on mimicking the structure and behavior of blood cells. Two basic themes emerge—the use of block copolymers to make polmer vesicles and the functionalization of colloidal or polymeric microspheres with cell-like adhesive properties. Both platforms provide a means for building the complex hierarchy that is characteristic of biological cells, while also incorporating novel and perhaps superior properties of material strength, specific targeting, and controlled release.

INTRODUCTION

Biological cells are complex, hierarchical materials. As such, they perform a number of functions that include self-propulsion, adhesion and arrest, evolution and differentiation, replication and division, as well as nutrient transport and secretion. Any recent text on cell and molecular biology vividly demonstrates such tasks and also emphasizes how much has been learned over the last decade about the structural and molecular basis of cellular function. From the materials point of view, physicochemical principles such as self-assembly in aqueous solution pervade modern cell biology. Recognition of such principles clearly suggests synthetic routes to cell mimicry and function. This brief review specifically focuses on two recent innovations in these directions that make selective use of modern materials and methods to engineer synthetic cells.

The field of artificial cells is not new. The first efforts were perhaps those of Chang (6) who microencapsulated the isolated contents of the simple red cell. The method used centered on inverse emulsification of the cellular material into an organic such as chloroform:cyclohexane, followed by stabilization of the dispersed droplets through addition of surfactant plus an interfacially accumulating polymer. The interfacial stabilization proved sufficient to allow separation of the cell-size droplets by simple centrifugation. The membrane that resulted was found to be semipermeable so that encapsulated cell enzymes such as carbonic anhydrase were found to act with reasonable kinetics on a permeating substrate. A reported

drawback to this classic approach was the unavoidable denaturation of protein at the interface with the continuous organic phase. As a consequence, it seems that the in vivo activity and survival of the microcapsules were limited by denatured surface proteins.

The early results of Chang and coworkers point to the fact that Nature tends to use a more molecularly structured approach to equilibrium self-assembly in aqueous media. Recognition of this feature presents challenges in chemical synthesis, some of which have been met in the last few years with the generation of, for example, block copolymers that self-assemble in water (21). Moreover, the ability to engineer enhanced activity into mimicking structures holds the promise to go beyond cells and make super-cellular materials for biological or medical applications. As Chang and coworkers recognized long ago, a number of opportunities exist in nutrient transport and drug delivery, as well as in other fields. As a specific example, the search for blood substitutes is strongly motivated by frequent blood shortages, as well as blood-borne contagions such as HIV and hepatitis C. Recognition of application, as well as opportunities in design and characterization of soft nano-structured materials, seems extremely likely to spur synthetic and physical chemists, as well as materials scientists, to produce novel molecules and materials for de novo cellular engineering.

In the spirit of an annual review, we briefly summarize recent work in the area of artificial blood cells, both red cells and white cells. Synthetic polymers constitute the basic material approach with added functionality achieved via attached biomolecules. Two specific accomplishments are reviewed and placed in context: the construction of encapsulating vesicles from amphiphilic block copolymers that self-assemble in water and the construction of polymeric microspheres that mimic the adhesion of white cells or leukocytes.

BIO-INSPIRED POLYMER MEMBRANES

Biomembrane Schematic: A Glycocalyx, Fluid Bilayer, and Solid Network

The central structural feature of a prototypical biomembrane is a lamellar bilayer of self-assembled lipids (Figure 1). Proteins invariably associate with the membrane, however, and these impart additional, critical bio-functionality. The proteins are either transmembraneous (with a portion inserted through part or all of the membrane) or peripheral (with only a small intercalation into the membrane and located on either the cytoplasmic or extracellular side of the membrane). On the outer face of the membrane is a "forest" of proteins that is extensively glycosylated and therefore high in oxygen content. In addition, on the cytoplasmic face of most biomembranes is a proteinaceous cytoskeleton that is anchored to the membrane via transmembrane proteins. From detailed studies of the simplest of cells, the red cell, properties of the membrane ranging from stability to compatability emerge as a composite of both the bilayer membrane and the underlying cytoskeleton, including how precisely the layers are connected. Whereas

the lipid bilayer constrains the overall size, i.e. area of the cell and establishes a semipermeable selective barrier (e.g. 27), the glycocalyx has both active and passive roles in cellular interactions, such as signaling, adhesion, and suppression of interactions. The network, in comparison, stabilizes the membrane against shear (reviewed recently in 31).

Self-Assembling Polymer Membranes

There is a well-recognized similarity between the overall structure of a biomembrane, in particular the lipid bilayer, and the lamellar phase often found in block copolymer melts and dispersions. This has led to various efforts to make self-assembled membranes from block copolymers, as summarized below.

POLYMER VESICLES FORMED IN SOLVENT-WATER MIXTURES When diluted into solvents such as *N*,*N*-dimethylformamide (DMF) and tetrahydrofuran (THF), many synthetic polymers have been found to form vesicle-like, sub-micron diameter structures. A recent example is a large polyethyleneoxide-polystyrene diblock copolymer of Yu & Eisenberg (40), EO*x*-PS*y* ($x = 15$, $y = 240$). This diblock forms vesicles when water is slowly added to organic solvent, and the precipitated structures appear stable after several days of dialysis into water. The spherical and deflated tubular vesicles that form have a wall thickness of 20–25 nm after being dried and metallized for transmission electron microscopy (TEM). This thickness is a small fraction of $PS_{240's}$ contour length of over 60 nm and suggests relatively unextended, perhaps entangled, core chains. Because of the very small hydrophilic PEO block in this particular synthetic, aggregates are said not to form directly in aqueous solution. A similar copolymer with $x = 45$ (or about 7% hydrophilic) generated an occasional vesicle at 1.5 wt% polymer in solution, but with $x = 80$ (or about 12% hydrophilic), no vesicles were generated. Replacing neutral PEO with polyacrylic acid (PAA) and using even longer PS chains (up to 500 units) also leads to vesicles in a solvent-selective manner, as reviewed extensively in Yu et al (41). Consistently, the resulting membranes ranged from 20 to 40 nm in thickness. In these systems it appears likely that the organic solvent is imbibed by the hydrophobic core, fluidizing it, lowering the glass transition of PS, and enabling sufficient topological rearrangement of a polymer lamellae to close upon itself and form at least sub-micron diameter spherical vesicles.

A structurally distinct synthetic that also makes vesicles is a pentablock of polyethyleneoxide-polymethylphenylsilane (PMPS-PEO)2-PMPS of 27 kDa (22). This copolymer is about 50% hydrophilic with a polydispersity of 1.6 (as the weight-to-number average molecular weight). This polydispersity is at the upper end of most reported vesicle-forming polymers described to date. The two PEO blocks were designed to cap, both inside and outside the vesicles, the stiff hydrophobic PMPS segments. The latter span the 8–12-nm-thick hydrophobic core revealed in negative-staining TEM. The finding that addition of bulk PMPS to water generated poor dispersions of a few small vesicles suggests that this design is almost lipid-like in its overall amphiphilicity.

Another recent and novel example of vesicle formation in solvent started with polyisoprene-*block*-poly(2-cinnamoylethyl methacrylate) (PI88-*b*-CEMA230) (11). Interestingly, cross-linking of the PCEMA shell and conversion of the PI chains to poly(2,3-dihydroxyl-2-methyl-butane) generated water-soluble and rhodamine-loadable nanospheres. Given the 230 monomers of the hydrophobic chain, a shell thickness for these structures of about 20 nm suggests an unusual, perhaps entangled, inner membrane structure. An even more recent example of a polymerizable polymer membrane started with poly(2-methyloxazoline)-poly(dimethylsiloxane)-poly(2-methyloxazoline) (PMOXA-PDMS-PMOXA) as a triblock of 9 kDa that was 40% hydrophilic (28). Vesicles were precipitated from ethanol with addition of water, and the two functional ends of each constituent chain were activated by ultraviolet light to polymerize the membrane. Solidity of the final membrane was primarily suggested by a collapsed, hollow sphere morphology observable under scanning electron microscopy.

POLYMER VESICLES THAT ASSEMBLE IN WATER A subset of polymer vesicles have now also been shown to assemble directly under solvent-free aqueous conditions just as lipid vesicles do. Among these super-amphiphiles that, as polymers in the conventional sense, are significantly larger than lipids is the chiral construct PS40-(isocyano-L-alanine-L-alanine)$_x$ (9). For $x = 10$, but not $x = 20$ or 30, small collapsed vesicles with diameters ranging from tens of nanometers to several hundred nanometers, and a bilayer thickness of 16 nm were observed by TEM to exist under mildly acidic conditions. Interestingly, bilayer filaments and superhelical rods were found to coexist under the same solution conditions, perhaps reflective of repulsive destabilization of the more planar membrane structures. However, comparatively neutral vesicles made in a range of aqueous media with polyethyleneoxide-polyethylethylene, specifically EO_{40}-EE_{37}, also coexist, although dominantly, with spherical and worm-like micelles (Figure 2*A*) (12). Once again, the membrane of these vesicles was found to be hyperthick: cryo-TEM resolved a hydrophobic core thickness of 8 nm. These PEO-PEE polymersomes are reviewed further below in relation to membrane properties. Very similar initial results with a polyethyleneoxide-polybutadiene (PEO-PBD) diblock have also been recently described (24a). Importantly, this non-hydrogenated precursor to PEE can be covalently cross-linked, thereby allowing a membrane elastic network to be established as highlighted in Figure 1.

Finally, a relatively conventional pluronic consisting mostly of polypropyleneoxide (EO_5-PO_{68}-EO_5; 10% PEO by weight) has also been reported to yield small vesicles observable by cryo-TEM (32). However, a mean vesicle half-life of only a few hours more than likely reflects the high oxygen content of the weakly hydrophobic polypropyleneoxide block. The relatively thin polymer membranes of 3–5 nm, compared with the 25-nm contour length of PO68, probably reflects a tendency for interfacial localization of the mid-block oxygen. By factoring this oxygen into the hydrophilic fraction, what unifies all of the above vesicle-forming

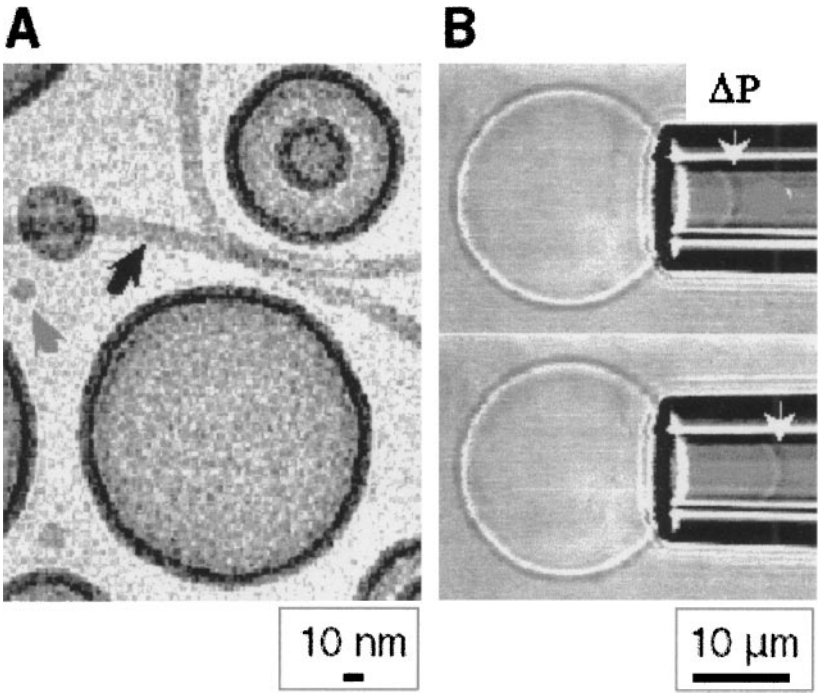

Figure 2 Polymer vesicle images (12). (*A*) Cryo-transmission electron micrograph (CTEM) of vesicles made of PEO-PEE. (*B*) Optical image of a giant polymersome. The PEO-PEE vesicle is suspended in aqueous solution (250-mM sucrose) and pulled into a micropipette by an increasing negative pressure, ΔP.

super-amphiphiles with natural lipids is a common hydrophilic weight or volume fraction in the range of 20 to 40%.

Micromaterial Characterizations

INTERFACIAL ELASTICITY AND PERMEATION TO RUPTURE: PROPERTIES OF PEO-PEE VESICLES

Because the stability of bulk copolymer mesophases is well-appreciated as depending on the product of the Flory interaction energy, χ, and chain length, N, one would expect that these same parameters underlie at least some measurable properties of polymer vesicles. For instance, as a relative measure of the dominant χ, the interfacial tension, γ_{HP}, at the membrane surface defined by the HP-block intersection ought to prove physically reasonable. In addition, given a similar χ as a lipid membrane, the relatively larger N of a polymer membrane ought to yield a more cohesive structure.

Membrane properties such as interfacial elasticity and membrane cohesiveness are directly accessible through measurements on giant, cell-sized PEO-PEE

vesicles (diameters >5 μm). Figure 2*B* shows a many-micron-sized vesicle (of radius R_s) being aspirated into a micropipette (of radius R_p): a negative pressure ΔP increases the membrane area by ΔA relative to the original vesicle surface area, A_0. A proportionality between the pressure-imposed surface tension, $\tau = 1/2\ \Delta P\ R_p/(1 - R_p/R_s)$, and relative area dilation, $\alpha = \Delta A/A_0$, yields an area elastic modulus, $K_a = \tau/\alpha$ with units of interfacial tension (Figure 3*A*). A value of $K_a \approx 120$ mN/m reported for PEO-PEE vesicles, together with the common view that $\gamma_{HP} = {}^1\!/_4\, K_a \approx 30$ mN/m, proves consistent with an H-P: oil-water interface. Importantly, the enhanced mean thickness, *d*, would appear to have no influence on this interfacial tension. This is consistent with a broad range in K_a for lipid membranes (from 100–1000 mN/m) (25) despite a very narrow range for d_{lipid}. In contrast, the bending elastic constant, K_b, that was reported to be $\sim$35 k_BT (12) appears extremely well approximated by an elastic plate model prediction of ${}^1\!/_{48}\, K_a\, d^2$, which is derivable for a bilayer of two uncoupled monolayers.

In spite of lipid-like elasticity, the stably sustainable critical strain, α_c, of the PEO-PEE vesicles (0.19 ± 0.02) considerably exceeds the range of 0.03–0.06 typical of natural lipid membranes (Figure 3*B*). Similar to bending and also membrane permeability (12), this cohesive stability (corresponding to $\sim$0.5 to 1 k_BT/nm^2) appears likely to have its origins in membrane thickness. Because K_a provides a measure of γ_{HP}, and γ_{HP} is related to χ, comparisons of α_c for different effective *N* ought to be made with membranes having similar K_a. The unsaturated lipid DAPC mixed with cholesterol (1:1) has a $K_a = 102$ mN/m, or $\gamma_{HP} \approx 25$ mN/m, (25), and it has an $\alpha_c = 0.043$. If a critical yield stress of $\sigma_c = K_a\, \alpha_c/d \approx 1$ MPa is postulated as common to both this particular but very representative lipid membrane and the PEO-PEE polymersomes, then one would naively expect both critical yield tensions and strains to increase linearly with membrane thickness. However, an estimate based linearly on *d* alone is simply too low; instead, a more hydrophilic pore would introduce the outer corona thickness, δ. The hydrated PEO chain is believed to extend $\delta \approx 4$ nm above each interface, whereas a lipid bilayer has a total thickness of 4–5 nm. A ratio of $(d + \delta)$ for the two systems allows rationalization of the rupture tension measured for the first polymer membranes.

Encapsulants and Complex Media Stability—Biomedical Directions

Complex solutions can modulate, and in particular undermine, the stability of polymer vesicles through mechanisms that, for example, reduce or change molecular packing. Indeed, difficulties in the encapsulation of globular proteins can arise with the surfactant-like character of denatured proteins, although the hydrated PEO brush of the present copolymers would tend to oppose interfacial access. The work of Chang (6) mentioned in the INTRODUCTION highlights the relevance of interfacial denaturation phenomena. It is nonetheless found with polymersomes that encapsulation can be as straightforward as adding solid pieces of bulk diblock to an aqueous solution of desired encapsulant and waiting 24 h

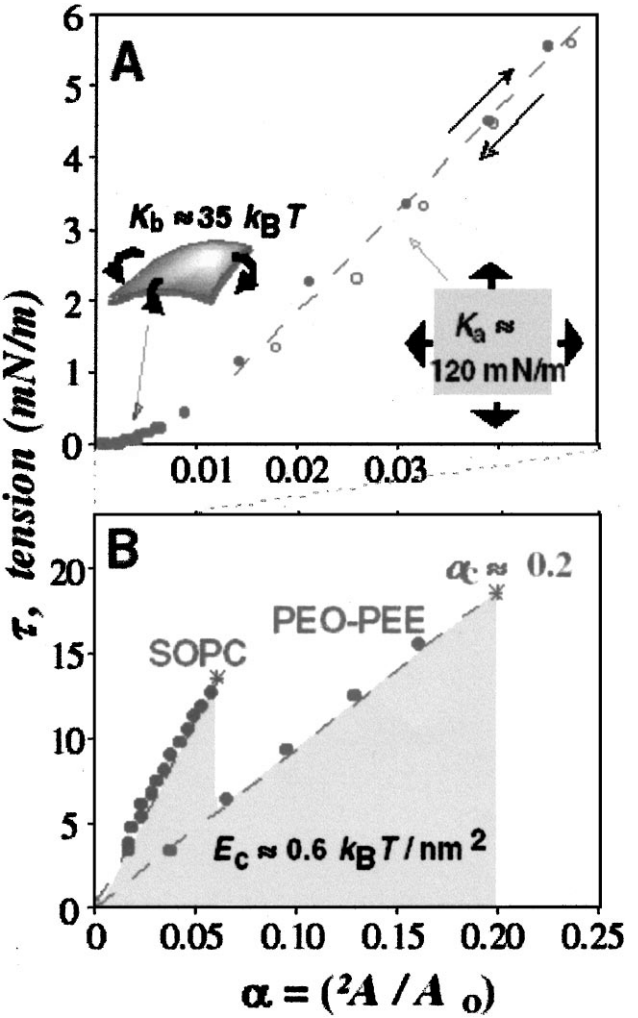

Figure 3 Micromechanical characterization of PEO-PEE vesicles by aspiration. (*A*) Relationship between the ΔP-induced tension, τ, and membrane expansion α, reveals the two invariant modes of deformation of a soft fluid membrane. These modes are illustrated in insets together with the corresponding elastic bending and area expansion moduli. (*B*) Membrane toughness was determined by aspiration to the point of rupture (asterisk). The figure demonstrates the difference in both critical area strain, α_c, and the cohesive energy density, E_c, between a common lipid vesicle, SOPC, and a PEO-PEE vesicle.

(24a). To develop a sense of encapsulation efficiency, three encapsulants were examined: myoglobin, hemoglobin, and albumin. All three proteins could be entrapped during vesicle formation, although the efficiency of encapsulation, as well as its limitations, has as of yet to be fully understood. Nonetheless, it is clear that encapsulation of macromolecules can be done with polymersomes.

More complex than a solution of a single protein, blood plasma has a number of surface-active agents, including fatty acids and carrier proteins. In addition, such colloidal entities generate osmotic depletion forces by becoming excluded from narrow gaps between juxtaposed membranes; surfactant bridging between adjacent vesicles can then act to more rigidly couple vesicles together. Stability in plasma thus has at least two aspects: membrane patency and colloidal stability. These polymer vesicles are found to be stable for at least five days in plasma when suspended at room temperature and kept well-mixed in a quasi-physiological manner (24a). Furthermore, colloidal stability is demonstrated out to almost 60 h in quiescent plasma; aggregation of settled-out vesicles occurs at longer times. However, polymersomes in the formed aggregates do not appear to coarsen into either giant vesicles or bulk lamellar phases, despite the close proximity and elevated density in the aggregates. This indicates that polymer membrane fusion is not readily achieved—a finding most likely attributable to repulsion by the PEO brush. Nonetheless, the dense aggregates are not exceedingly fragile assemblies either because they could not be sheared apart by rapid dragging through solution and generated surface shear stresses as high as $\sim$1 dyne/cm^2. Regardless, the likelihood of forming such aggregates in vivo seems remote owing to incessant fluid motion.

Interactions with Biological Cells: Phagocyte Challenge In Vitro

With polymersomes at least partially stable in blood plasma, a logical next step was to assess the interaction of a polymersome with the cellular components of blood, particularly granulocytes, which are the predominant circulating phagocytes. The basic in vitro experiment is illustrated in the video excerpts of Figure 4, which show either a yeast particle or a polymersome being brought into contact with blood cells. When placed in contact with a red cell, neither a polymersome nor a yeast particle exhibits any adhesion or other clear cellular response, despite the presence of 20% plasma. In comparison, 1–2 min of contact between a yeast particle and a white cell (known as a neutrophil or differentiated leukocyte) leads to strong adhesion. This generally develops further as the white cell spreads and actively engulfs the yeast particle (Figure 4*A*, *left*). This type of control experiment was generally complete within 3 to 4 min ($n = 3$ particles) (Figure 4*B*) and was found to occur even faster at 37°C. In contrast, over the same length of time and much longer, PEO-PEE polymersomes appeared inert to these phagocytic cells ($n = 5$ vesicles). Several such experiments are summarized in the timelines of

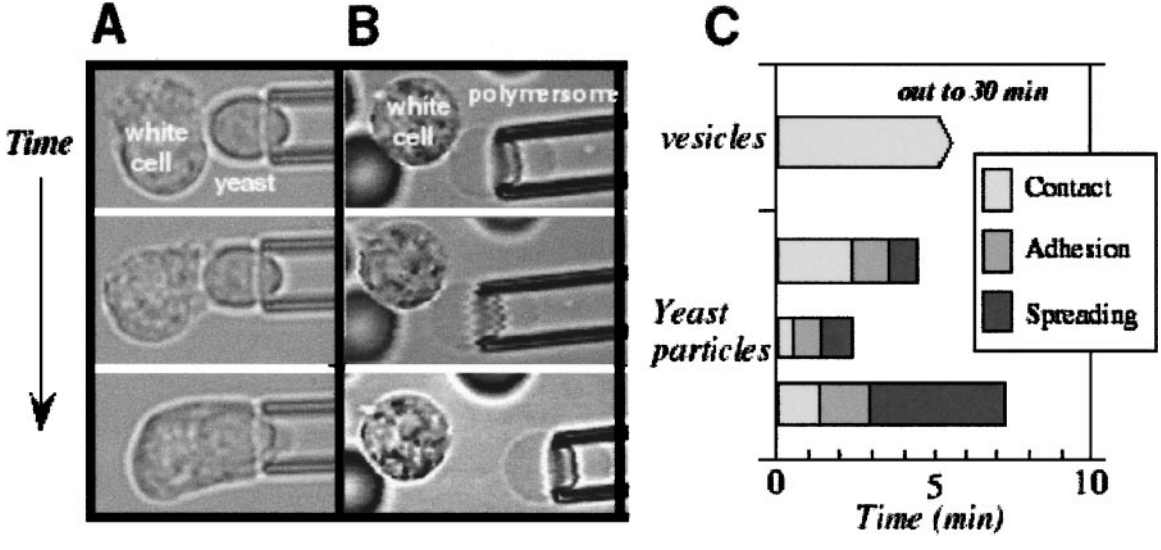

Figure 4 Phagocyte challenge in vitro. Yeast particles (*A*) or PEO-PEE polymersomes (*B*) were mixed in 20% citrated plasma and manipulated into contact with freshly isolated and washed white blood cells or red blood cells. (*C*) Within about 5 min, white cells adhered to and engulfed the yeast particles, consistent with earlier studies (42). Polymersomes appeared inert in contact with a white cell for as long as 30 min. Interactions with red cells were non-existent as well. The micropipette inner diameter is 5 μm. Experiments shown were done at room temperature and lasted 30–60 min in total duration.

Figure 4*C*. Results similar to those for PEO-PEE were also found with EO_{26}-BD_{46} (BD = butadiene), at least out to 5–10 min, despite this second polymer's shorter PEO chain of about only 1 kDa.

Similar in vitro tests of polymersomes with macrophages (another differentiated type of leukocyte) as well as more quiescent cells, including endothelial cells and myoblasts, further indicate the inertness of the polymersome surface. The dense PEO brush of the polymersomes seems to act like the glycocalyx on cellular exofaces, preventing the deposition of phagocytic ligands such as plasma C3b on the vesicle surface and/or repelling phagocyte adhesion. The in vitro protein-rejecting properties of PEO-coatings, including nanoparticles (30), are well-appreciated (23). Ultimately, the lack of polymersome recognition by phagocytes would seem important to prolonged circulation upon intravital injection. Emerging studies involving intravenous injections of ~100-nm vesicles into rats appear to substantiate this conjecture.

Cross-Linked Polymersome Membranes

Most recently, the double bonds embedded in the hydrophobic core of PEO-PBD have allowed us to fully cross-link the membrane of giant unilamellar vesicles (BM Discher H Bermudez, Y-Y Won, DA Hammer, FS Bates & DE Discher, submitted). This has been attempted for decades with lipids but without success (H Ringsdorff, personal communication). We speculate that this is because polymerization strains the nanostructure (39) and lipids cannot handle the strain, whereas polymersomes can. This problem is exacerbated by the low number of available sites for cross-linking that have been tried in lipid systems. It is clear that the cross-linked polymer membranes are imparted with a shear rigidity that makes them respond in deformation similar in quality, most notably, to red cell membranes (see Figure 1). Hence, the development of hemo–polymersomes that have material properties of red cells and encapsulate oxygen-binding globins is rapidly emerging.

BIOADHESIVE COLLOIDS

Leukocyte Adhesion

A second approach to using synthetic materials to recreate the dynamic function of biological cells has been the development of chemically derivatized particles that recreate the dynamics of leukocyte adhesion. In physiology, cells in the circulation must traffic from blood into tissues. To do this, cells must adhere to blood vessel walls via specific receptor-ligand binding. Many cells exhibit this type of adhesive trafficking, such as leukocytes (as part of their physiological function of entering tissue to eliminate invaders), stem cells (which leave blood vessels and enter bone marrow to proliferate and differentiate to give rise to blood cells), and tumor cells (during metastasis, in which they enter the circulation to spread throughout the

body). Therefore, adhesion of blood borne cells to blood vessel walls is a ubiquitous physiological process.

By far, the best studied of these processes is leukocyte trafficking, and although our knowledge of the surface molecules involved in this type of adhesion is not complete, there has been some definitive elucidation of which adhesion molecule pairs participate in leukocyte trafficking. Interestingly, the trafficking of white cells out of the circulation occurs in two steps (for a more complete but recent review, see 14). The first step, called rolling, is a dynamic friction in which the white cell is slowed down but not stopped by interactions with the endothelial cells that line the blood vessel wall. This step is mediated by very specialized molecules, including selectins and their ligands, as well as the integrin heterodimer $\alpha_4\beta_7$. Rolling is followed by firm adhesion, which in leukocytes is mediated by integrin heterodimers in the β_2 family. β_2 integrins must undergo a complex structural change to enter a state where it can bind strongly with its ligand (typically a member of the Ig superfamily), which then leads to firm adhesion. This structural change is induced by signal transduction pathways within cells, which are initiated through either the occupancy of selectin molecules during rolling or the binding of chemokine ligands to chemokine receptors on cells (14).

The recreation of the rolling step of the adhesion cascade using synthetic chemistry has immense value in both understanding how adhesion works and also designing cellular mimetics that can target and exploit the same pathways that cells use to traffic throughout the body. It is not clear which leukocyte cell surface receptors actually mediate rolling adhesion on endothelium. The uncertainty comes from the fact that selectins are selective lectins; (*a*) lectins are proteins that bind to carbohydrates, and (*b*) the carbohydrate decorations on a single protein scaffold can vary widely. Each selectin appears to respond to different carbohydrate decorations, which in turn are presented on different protein backbones on cells. One common feature of all selectin ligands is the requirement for a sialylated-fucosylated carbohydrate ligand, such as sialyl-Lewis^x. These carbohydrates are often linked to hydroxyl groups on threonines or serines (thus described as *O*-linked glycosylation). The carbohydrate decorations may act in concert with other structural features of the selectin ligand. For example, P-selectin glycoprotein ligand-1 (PSGL-1), which is found on leukocytes and which supports rolling on P-selectin, has a threonine at position 16 that is glycosylated, but it has been postulated that tyrosine sulfation is also required for full PSGL-1 activity (26). Therefore, sialyl-Lewis^x, or a closely related carbohydrate, can be viewed as the minimum functional binding element of the selectins (17). The current view of receptor-ligand biochemistry that supports leukocyte rolling adhesion is shown in Figure 5.

The location in the vasculature where leukocytes bind is controlled by the expression of ligands (selectins or selectin ligands) on the upper surface of endothelial cells that line blood vessels. Endothelial cells can express both P- and E-selectin, in response to cues it receives from the environment. The control of leukocyte recruitment in inflammation (when there is an infection in tissue) is through the

generation of tissue factors (cytokines), released from survelliance cells, that cause endothelial cells to express E- and P-selectin, thus recruiting white cells.

After rolling, leukocytes bind firmly through firm adhesion mediated by the β_2 integrins binding to molecules in the Ig superfamily (intercellular adhesion molecule-1, ICAM-1).

Leukocyte Mimics

The fact that all three selectins share a common carbohydrate epitope, sialyl-Lewis^x as a ligand (17), led to the first cell-free colloidal mimetics of leukocyte adhesion. The strategy behind construction of colloidal mimetics to leukocyte adhesion is shown in Figure 6. Biotinylated forms of sialyl-Lewis^x were bound to streptavidin-coated polystyrene microspheres, and their adhesion was measured on E-selectin-coated surfaces under shear flow in a parallel plate flow chamber (3, 4). Slow rolling, defined as rolling of several to tens of microns per second at shear stresses up to 2 dynes/cm^2, as seen for leukocytes on endothelium or purified E-selectin surfaces (24), was observed. Cellular rolling is also distinguished by a variance in the rolling velocity (fluctuation in instantaneous velocity about its average value); this dynamic feature of the rolling was also observed with the cell-free system (3, 4). The rolling was specific because antibodies against sLe^x or E-selectin fully inhibited the rolling. The rolling of sLe^x-coated spheres on E-selectin, and the close similarity in rolling dynamics between the reconstituted microspheres and neutrophils indicated that receptor-ligand physical chemistry was responsible for the control of neutrophil adhesion and suggested that features such as cell deformability, roughness, and intracellular signaling were not determinants of neutrophil rolling dynamics. These results seemed to explain the ability of glutaraldhyde-fixed neutrophils to roll E-selectin-coated surfaces (16).

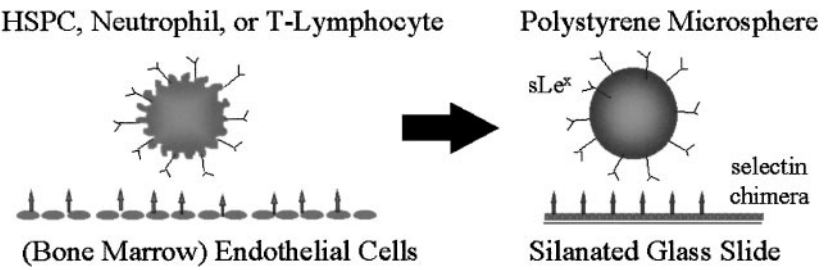

Figure 6 In cell-free systems, the adhesion of leukocytes (lymphocytes or neutrophils) and hematopoietic stem and progenitor cells to endothelial cells can be recreated by attaching small molecule ligands (parts of selectin adhesion ligands) to microspheres. The endothelium can be recreated by attaching endothelial surface molecules (such as E- and P-selectin) to glass slides. The dynamics of adhesion displayed by these microspheres interacting with selectin-coated surfaces, as measured in a flow chamber, closely approximates that of leukocytes adhering to endothelium under flow.

Subsequently, rolling was also observed using sLe^x-coated beads on both P- and L-selectin surfaces (31, 19 respectively). The result for P-selectin was informative because it had been previously thought that PSGL-1, the ligand for P-selectin, had to be both glycosylated and tyrosine-sulfated for rolling activity (26). However, sLe^x-coated beads showed robust rolling on P-selectin (31). The rolling dynamics of sLe^x-beads on P-selectin could be compared to that engineered with PSGL-1-coated beads. The ability of PSGL-1-coated spheres to adhere to P-selectin-coated surfaces under flow was first shown by Goetz and coworkers (18). In our experiments, a chimeric form of PSGL-1, containing the last N-terminal 19 amino acids of PSGL-1 linked to the Fc portion of a human IgG_1, was attached to protein A-coated microspheres as the same density at which PSGL-1 is found on human neutrophils. The rolling of neutrophils, sLe^x-coated spheres, and PSGL-1-coated spheres could be compared (Figure 7*B*). Neutrophils rolled the slowest, PSGL-1-coated spheres rolled only slightly faster, and sLe^x-coated spheres rolled the fastest but still displayed robust rolling. These results indicate again that roughness, deformabilty, and signaling have a limited effect on the dynamics of cell rolling (because PSGL-1-coated beads closely approximate the rolling of neutrophils) and that tyrosine sulfation enhances but is not necessary for robust rolling on P-selectin (sLe^x-beads do display adequate rolling on P-selectin).

This latter point remains a controversy in the selectin field because mutation of all the tyrosine to phenyalanines in PSGL-1 expressed in a cellular system seems to abolish rolling on P-selectin (26). Further experiments with purified amino acids from the terminal 19 amino acids of PSGL-1 indicate that peptides that are glycosylated but not sulfated do support rolling on P-selectin (31), consistent with the previously-cited result that sLe^x-coated beads support rolling on P-selectin. One self-consistent explanation for this apparent discrepancy is that PSGL-1 in which tyrosine is mutated to phenyalanine may be improperly processed and glycosylated in cellular systems, which further argues for testing the chemical dependence of rolling using systems that involve molecular synthesis and reconstitution for recreation of proper activity.

On L-selectin, sLe^x-beads could be used to recreate the rolling that had been observed in cellular systems using L-selectin and some of its carbohydrate-bearing physiological ligands. L-selectin-mediated rolling is much faster than that seen with the other selectins, presumably because of the faster off-rates of L-selectin with the carbohydrate (15). Rolling velocities observed with beads were in the high tens to hundreds of microns per seconds, and thus could be viewed as a fast skipping of the beads over the surface. The rolling velocity decreased with increasing L-selectin surface density (Figure 8*B*).

An interesting dynamic feature of L-selectin-mediated rolling is the shear threshold effect. The shear threshold effect describes the increase then decrease in adhesion as the shear rate increases, which is seen with L-selectin-mediated cell adhesion. It was first identified with neutrophils (which bear L-selectin) on peripheral-node addressin (PNAd) surfaces (PNAd is an sLe^x-bearing ligand found on endothelium in immune organs such as lymph nodes) (15). The maximum in

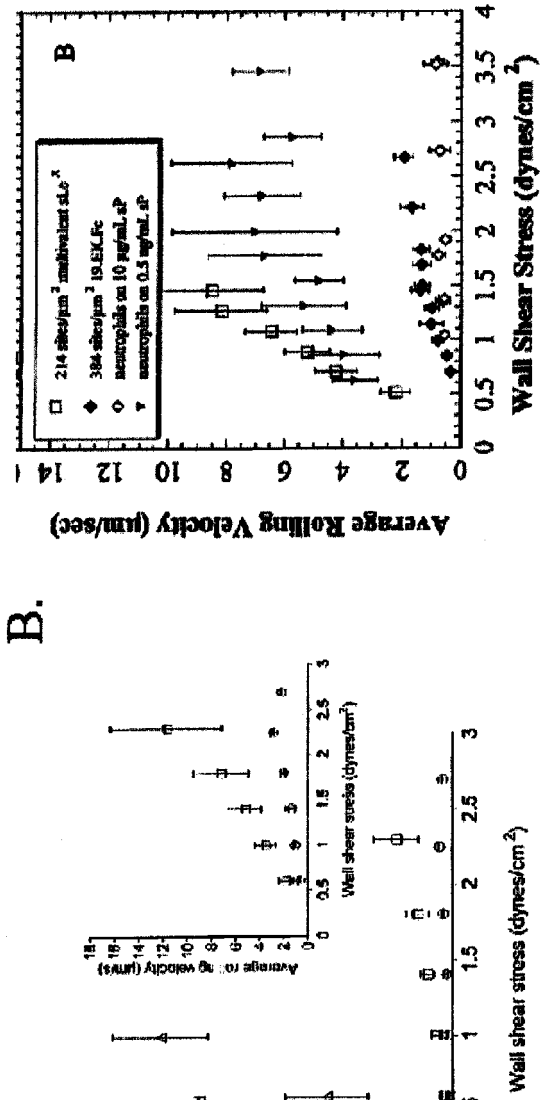

Figure 7 Data on the adhesion of carbohydrate and ligand-coated microspheres to selectin-coated glass slides using the cell free system. (*A*) Data on the rolling of beads coated with sLe^x, sialyl-Lewis^a (an isomer of sLe^x), and HSO_3-Le^x on E-selectin-coated surfaces under flow show that sLe^x or sLe^a-coated spheres roll at velocities of several microns per second over wall shear stresses up to 2.5 dynes/cm^2. HSO_3-Le^x-coated beads show weak adhesion on E-selectin, and sLe^a is a slightly better ligand than sLe^x for E-selectin. Thus the cell free system can distinguish fine differences in carbohydrate chemistry (3). (*B*) Cell-free rolling of beads on P-selectin. The adhesion of beads coated with sLe^x or a chimera of PSGL-1 (19.EK.Fc, which has the last 19 amino acids of PSGL-1 tied to the Fc portion of human IgG_1 via an enterokinase susceptible domain) were compared with neutrophils for adhesion under flow to P-selectin physiosorbed to glass slides. PSGL-1 coated beads (closed diamonds) roll almost as slowly as neutrophils (open diamonds). SLe^x-coated spheres roll significantly, but much more quickly than neutrophils (open squares), suggesting that PSGL-1 has features beyond sialyl-Lewis^x, which facilitate rolling (31).

adhesion, as measured by adhesion flux–number of adherent particles bound per unit time per area—is typically between 0.7 and 1 dyne/cm^2 (see Figure 8*A*) (15). It has now been shown that the shear threshold effect could be recreated in a cell-free system using sLe^x-containing beads on L-selectin-coated surfaces (19) (Figure 8*C,D*). The existence of the maximum seems to depend on the density of L-selectin. On high densities of L-selectin (as found with L-selectin densities created by physisorption with 5 μg/ml L-selectin), adhesion of sLe^x-coated beads steadily decreased with increasing shear stress. However, on lower densities of L-selectin, adhesion clearly goes through a maximum with shear stress (19). The effect of ligand density in controlling the shear threshold had not been observed before these experiments. Although a number of hypotheses for the control of the shear threshold effect have been postulated (cell roughness and micron-scale deformability, for example), it is clear from these cell-free adhesion experiments that the origin of the shear threshold must be in the physical chemisty of L-selectin binding its ligand. Hints of the shear threshold phenomena have also been observed in cellular aggregation experiments (33) and in antibody-antigen adhesion (35); it appears to be a fundamental phenomenon that governs molecular association for tethered receptors and ligands, and cell-free systems can help with its further elucidation.

Other Adhesive Systems

Leukocyte rolling, or dynamic friction, is a unique dynamic state of adhesion. As mentioned before, relatively few molecules support this type of adhesion. One can question what the functional properties of adhesion molecules need to be to generate this dynamic state of adhesion, and whether the same dynamics can be achieved with other molecules. This question has been extensively explored with antigen-antibody pairs whose affinities are chosen to match those of selectin-carbohydrate interactions. Some transient adhesion has been observed with low-affinity antigen-antibody interactions, but in general it is short-lived and either leads to no adhesion or firm adhesion (thus the transient or rolling adhesion is meta-stable). For example, Chen and coworkers showed that neutrophils adhere transiently to an antibody against sLe^x immobilized in a flow chamber, but the rolling was not sustained, was observed only with a period of pre-incubation, and was not observed at shear stresses above 1 dyne/cm^2 (7). Swift showed that antibody-mediated binding of rat basophilic leukemia (RBL) cells to antigen-coated surfaces was transient, but always ended in firm adhesion, for an antibody whose K_d for its antigen was within an order of magnitude of that for selectin-carbohydrate interactions (35, 37). Other very low–affinity pairs gave rise to either no adhesion or firm adhesion, but no state in between (36, 38). A possible explanation for the failure of these molecular systems to match rolling response is that adhesion dynamics depends on functional parameters that describe their binding other than affinity. Using computer simulations, it has been shown that the dynamics of adhesion might depend most closely on the mechanico-chemical properties of adhesion molecules or the dynamics of

their failure in response to force (5, 10, 20), as first postulated by Bell (1). In addition to the kinetics of dissociation, a bond's sensitivity to force has been predicted to govern the adhesive response of cells. Thus molecular interactions that have the same affinity as selectin-carbohydrate interactions would not necessarily give rise to the same dynamics of adhesion because the mechanico-chemical properties are not set by the affinity and are not necessarily the same.

Targeting Applications

Recently, the technology to make functional leukocyte mimetics has recently been extended with the clear goal of targeting for biomedical applications. Goetz' laboratory has shown that nanospheres coated with antibodies against P- and E-selectin can bind to these substrates under flow (2). Gimbrone's laboratory showed that vesicles functionalized with an antibody against E-selectin could be targeted to an inflammatory site in mice (34). It has been shown that small microspheres coated with PSGL-1 roll in vessels induced to express P- or E-selectin (or both) in mice (29).

A further development in this area is to combine the well-established technologies for making biodegradable microspheres from polymers, such as polylactic-glycolic acid (PLGA), with cell-free rolling and adhesion (8). Goetz and coworkers showed that biodegradable microspheres physisorbed with antibodies to E- and P-selectin showed limited, weak adhesion under a limited set of shear stresses to E- and and P-selectin surfaces. Recently, the Hammer laboratory has shown that sLe^x can be coupled to streptavidin-derivatized PLGA microspheres and that these spheres can roll on P- selectin surfaces (Figure 9). It is well known that such particles can be used for long-time–scale release of biological agents (8), and combined with functionalization that mimics the adhesive behavior of leukocytes, they may provide a useful tool for drug delivery, especially in inflammatory applications.

IMMEDIATE POSSIBILITIES

Clear avenues of future effort in synthetic cells lie in the engineering of polymersomes with specifically designed adhesive functionality. Surface groups on the polymer have already been derivatized with specific ligands such as biotin, allowing the hierarchical design of a wide array of adhesive functionality. Leukopolymersomes would provide the dual control of adhesion, through the selection of the type and density of leukocyte adhesion ligand, and synthetic cell rheology, through the selection of polymer type, length, and enacapsulant.

ACKNOWLEDGMENTS

The authors are grateful for the support of the Penn MRSEC (DMR-9632598) and NASA Materials Science program. Synthesis of block copolymers by Frank

Bates' group at the University of Minnesota is very gratefully acknowledged. The authors acknowledge the scientific contributions of B Discher, Y-Y Won, H Bermudez, C-M Lee, S Rodgers, D Brunk, D Tees, A Greenberg, M Santore, and L Eniola.

LITERATURE CITED

1. Bell GI. 1978. *Science* 200:618–27
2. Blackwell JE, Dickerson JB, Berg EL, Goetz DJ. 2001. *Ann. Biomed. Eng.* Submitted
3. Brunk DK, Goetz DJ, Hammer DA. 1996. *Biophys. J.* 71:2902–7
4. Brunk DK, Hammer DA. 1997. *Biophys. J.* 72:2820–33
5. Chang K-C, Tees DFJ, Hammer DA. 2000. *Proc. Natl. Acad. Sci. USA* 97:11262–67
6. Chang TMS. 1964. *Science* 146:524–25
7. Chen SQ, Alon R, Fuhlbrigge RC, Springer TA. 1997. *Proc. Natl. Acad. Sci. USA* 94:3172–77
8. Cohen S, Yoshioka T, Lucarelli M, Hwang LH, Langer R. 1991. *Pharm. Res.* 8:713–20
9. Cornelissen JJLM, Fischer M, Sommerdijk NAJM, Nolte RJM. 1998. *Science* 280:1427–30
10. Dembo M, Torney DC, Saxman K, Hammer DA. 1988. *Proc. R. Soc. London Ser. B* 234:55–83
11. Ding J, Liu G. 1998. *J. Phys. Chem. B* 102:6107–13
12. Discher BM, Won Y-Y, Ege DS, Lee JC, Bates FS, et al. 1999. *Science* 1284:1143–46
13. Discher DE. 2000. *Curr. Opin. Hematol.* 7:117–22
14. Ebnet K, Vestweber D. 1999. *Histochem. Cell Biol.* 112:1–23
15. Finger EB, Puri KD, Alon R, Lawrence MB, von Andrian UH, Springer TA. 1996. *Nature* 379:266–69
16. Finger EB, Bruehl RE, Bainton DF, Springer TA. 1996. *J. Immunol.* 157:5085–96
17. Foxall C, Watson SR, Dowbenko D, Fennie C, Lasky LA, et al. 1992. *J. Cell Biol.* 117:895–902
18. Goetz DJ, Greif DM, Ding H, Camphausen RT, Howes S, et al. 1997. *J. Cell Biol.* 137:509–19
19. Greenberg AW, Brunk DK, Hammer DA. 2000. *Biophys. J.* 79:2391–402
20. Hammer DA, Apte SM. 1992. *Biophys. J.* 63:35–57
21. Hillmyer MA, Bates FS. 1996. *Macromolecules* 29:6994–7002
22. Holder SJ, Hiorns RC, Sommerdijk NAJM, Williams SJ, Jones RG, Nolte RJM. 1998. *Chem. Commun.* 14:1445–46
23. Lasic DD, Papahadjopoulos D, eds. 1998. *Medical Applications of Liposomes*. Amsterdam: Elsevier. 794 pp.
24. Lawrence MB, Springer TA. 1991. *Cell* 65:859–73

24a. Lee JC-M, Bermudez H, Discher BM, Sheehan M, Won Y-Y, et al. 2001. *Biotech. Bioeng.* 73:135–45

25. Lipowsky R, Sackmann E, eds. 1995. In *From Cells to Vesicles*, pp. 1–5A. Amsterdam: Elsevier Sci. Vol. 1A
26. McEver RP, Cummings RD. 1997. *J. Clin. Invest.* 100:S97–103
27. Mohandas N, Evans EA. 1994. *Annu. Rev. Biophys. Biomol. Struct.* 23:787–818
28. Nardin C, Hirt T, Leukel J, Meier W. 2000. *Langmuir* 16:1035–41
29. Norman KE, Katopodis AG, Thoma G, Kolbinger F, Hicks AE, et al. 2000. *Blood* 96:3585–91

30. Peracchia MT, Harnisch S, Pinto-Alphandary H, Gulik A, Dedieu JC, et al. 1999. *Biomaterials* 20:1269–75
31. Rodgers SD, Raymond T, Camphausen RT, Hammer DA. 2000. *Biophys. J.* 79:694–706
32. Schillen K, Bryskhe K, Mel'nikova YS. 1999. *Macromolecules* 32:6885–88
33. Simon SI, Neelamegham S, Taylor A, Smith CW. 1998. *Cell Adhesion Commun.* 6:263–76
34. Spagg DD, Alford DR, Greferath R, Larsen CE, Lee KD, et al. 1997. *Proc. Natl. Acad. Sci. USA* 94:8795–800
35. Swift DG. 1998. *The extent and rate of antigen-antibody mediated adhesion of rat basophilic leukemia cells to surfaces in a linear shear field*. PhD thesis. Univ. Pennsylvania. 340 pp.
36. Swift DG, Posner RG, Hammer DA. 1998. *Biophys. J.* 75:2597–611
37. Swift DG, Posner R, Hammer DA. 2001. *Biophys. J.* In revision
38. Tempelman LA, Hammer DA. 1994. *Biophys. J.* 66:1231–43
39. Won YY, Davis HT, Bates FS. 1999. *Science* 283:960–63
40. Yu K, Eisenberg A. 1998. *Macromolecules* 31:3509–18
41. Yu YS, Zhang LF, Eisenberg A. 1998. *Macromolecules* 31:1144–54
42. Evans E. 1989. *Cell Motil. Cytoskelet.* 14(4):544–51

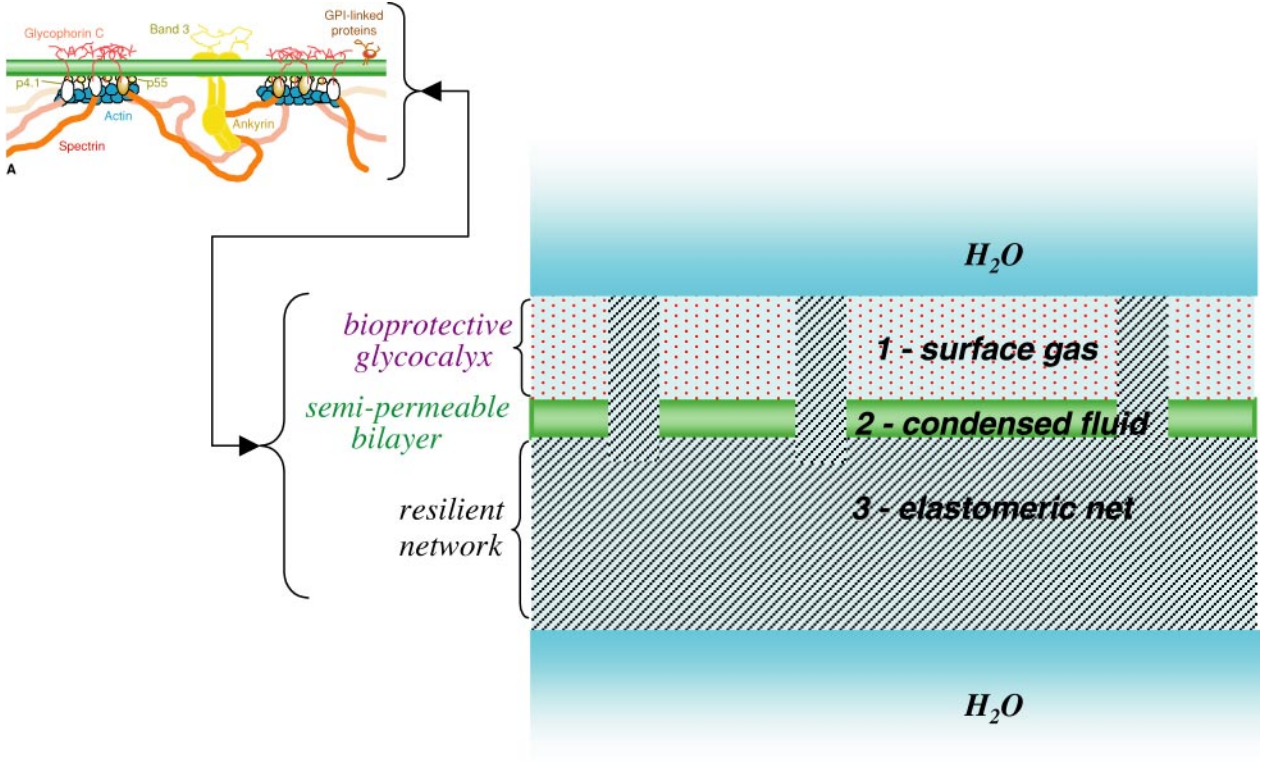

Figure 1 Typical biomembrane (13) and its coarse-grained, trilaminate representation.

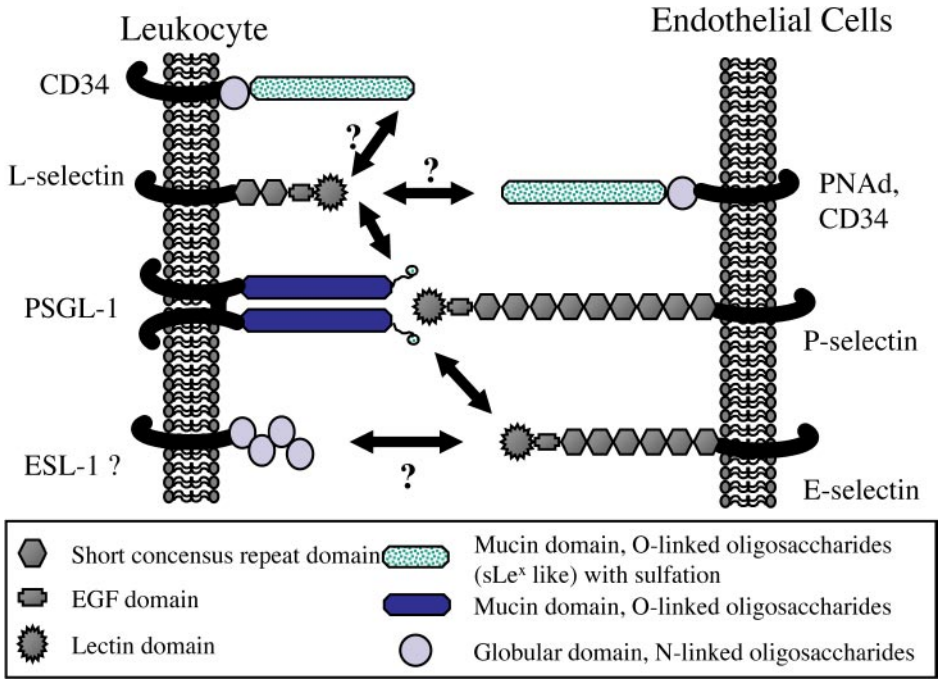

Figure 5 Adhesion molecules in the immune system used during leukocyte adhesion to endothelium. Selectin family molecules exist on leukocytes (L-selectin) and on endothelium (P- and E-selectin). Each binds to carbohydrate-bearing ligands, principally with O-linked glycosylation domains that bear the sialyated-fucosylated ligands sialyl-Lewis^x (sLe^x). L-selectin binds to peripheral node addressin and CD34; P-selectin binds to leukocyte P-selectin glycoprotein ligand-1 (PSGL-1); and E-selectin binds E-selectin ligand-1 (ESL-1). Other important structural domains include the EGF domain and consensus-binding repeat motifs on selectins and globular and mucin domains on selectin ligands.

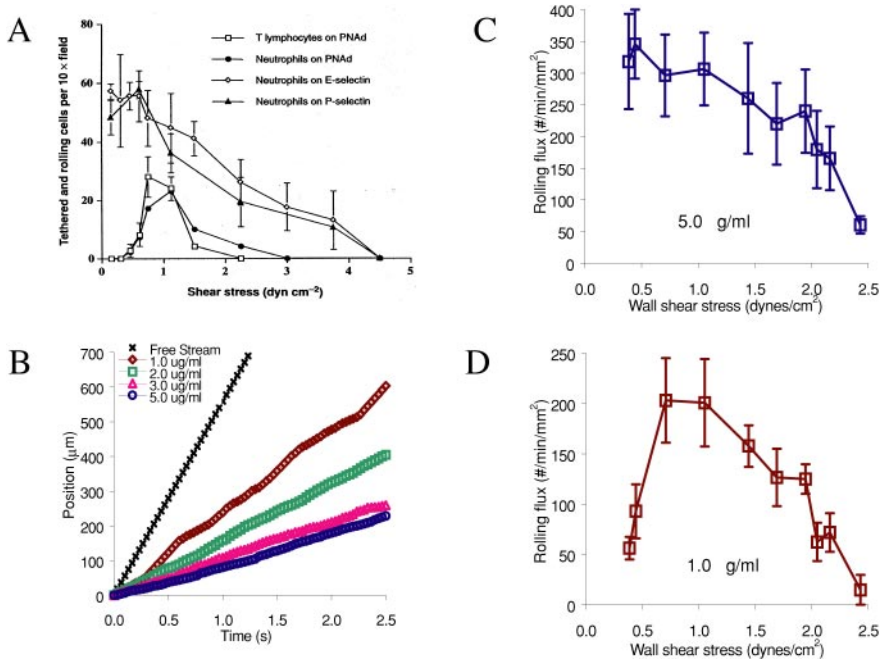

Figure 8 The shear threshold effect. (*A*) Neutrophils and lymophocytes were perfused over PNAd addressin, E-selectin, or P-selectin-coated surfaces under flow. On PNAd surfaces (where adhesion was mediated by leukocyte L-selectin binding to PNAd), there was a clear maximum in the adhesion with the shear stress. This maximum, not seen during adhesion via E- and P-selectin, is the shear threshold effect [reprinted by permission from *Nature* © 1996 Macmillan Mag. Ltd. (15)]. (*B*) sLe^x-beads roll over L-selectin-coated surfaces under flow. Increasing the density of L-selectin decreases the rolling velocity below that of a free stream particle (L-selectin concentrations are given as solution concentrations) (19). (*C*,*D*) Adhesion flux of sLe^x-coated beads on L-selectin shows a recreation of the shear threshold effect with a cell-free system at low, but not high, densities of L-selectin (19).

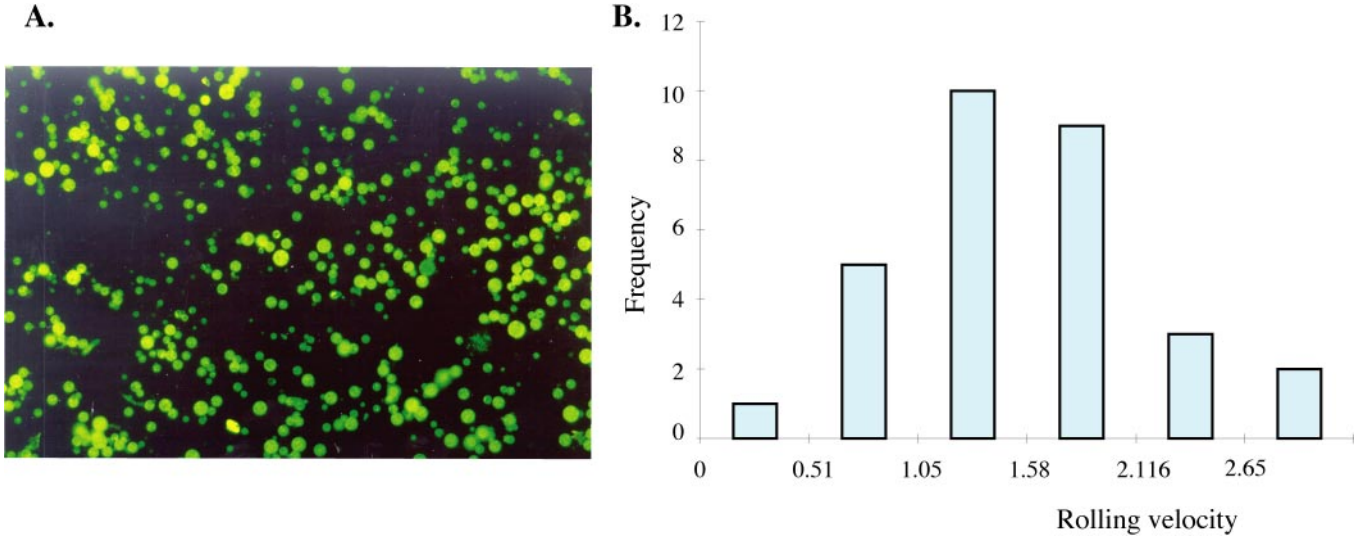

Figure 9 Cellular mimetics can be modified for potential drug delivery. (*A*) Micron-sized microspheres made from polylactic-glycolic acid polymers can encapsulate carboxyfluorescein, as viewed with a fluorescence microscope. (*B*) PLGA microspheres, covalently linked via carbodiimide with neutravidin, then decorated with biotin-SLe^x, roll on P-selectin-coated surfaces under flow, with rolling velocities in several microns/second. Heterogeneity in rolling velocity is the result of both heterogeneity in bead size (between 1 and 7 μm) and differences in sLe^x density. The shear stress was 1.235 dynes/cm^2, and the average amount of sLe^x/bead was 1.2×10^{-6} μg.

Annual Review of Materials Research
Volume 31, 2001

CONTENTS